Rheological Study of Chain Dynamics in Dilute Binary Polymer Mixtures

Shanfeng Wang, Yaseen Elkasabi, and Shi-Qing Wang*

Maurice Morton Institute of Polymer Science and Department of Polymer Science, The University of Akron, Akron, Ohio 44325

Received May 25, 2004; Revised Manuscript Received October 18, 2004

ABSTRACT: Recent progress toward a more realistic understanding of chain dynamics in entangled binary mixtures has prompted us to examine in detail the nature of probe chain dynamics in binary mixtures in the dilute limit. We have carried out theoretical analyses to determine the solution rheological signatures of various types of chain dynamics and subsequently performed rheological measurements on a number of binary mixtures. We found in general agreement with the theoretical predictions that there are indeed several interesting regions including the familiar Zimm solution behavior, the Rouse-like solution behavior for both nonentangled and entangled matrices, and a Stokes-sphere dynamics involving a probe chain in a well-entangled "solvent". These experimental results reveal a high level of interplay between the probe and matrix chain lengths that dictates the actual probe chain dynamics. For example, a longer matrix chain is more effective in screening both excluded volume and hydrodynamic interactions and in delaying the onset of the nonlinear concentration dependence of the zero-shear solution viscosity.

I. Introduction

The reptation theory for entangled chain dynamics appears to offer a satisfactory account of the experimental observations for monodisperse polymer samples upon incorporation of the contour length fluctuation (CLF) effect and constraint release (CR) effect.[1−6] In particular, the deviation of 3.4 from the reptative exponent 3.0 for the chain relaxation time τ_d and zero-shear viscosity η_0 has been suggested[6,7] to arise primarily from the CLF. The polymer mode coupling theory, however, suggests that the CR instead of the CLF plays a dominant role in affecting both diffusion and stress relaxation behavior.[8] We have recently noted that the tracer/trace diffusion coefficient appears to scale with the probing chain molecular weight M_w as $D_{tr} \sim M_w^{-2.0}$as one would anticipate from the original reptation idea without CR and CLF effects, whereas the self-diffusion coefficient scales nonideally like $D_s \sim M_w^{-2.4}$ but also converges onto $D_{tr} \sim M_w^{-2.0}$ for $M_w \gg M_e$, with M_e being the entanglement molecular weight.[9,10] If CLF is allegedly the cause[7,11,12] for the scaling of D_s to deviate from $M_w^{-2.0}$, it should also cause D_{tr} to scale nonideally, unless the presence of a higher molecular weight matrix in tracer/trace diffusion measurements introduces some unspecified hindrance effect to cancel the CLF effect. On the other hand, we are constantly reminded of the two computer simulation studies[13,14] claiming that D_{tr} would scale nonideally with M_w. The CR is even more important for blends made of a trace amount of long chains embedded in a matrix of shorter chain length. Many previous studies have elucidated the CR effect by either diffusion and rheological measurements[15−18] or computer simulations.[19]

Apart from the special conditions of monodisperse melts and dilute limits of one chain length in a matrix of a different chain length, there is an equally important case of binary mixtures where a significant fraction of one chain length is in the presence of another. Study of chain dynamics in these binary mixtures is the first step toward a reliable description of rheological behavior of polydisperse samples.[10,20−24] Recently we have made some progress toward this goal by carrying out both rheological and diffusion measurements of 1,4-polybutadiene binary mixtures where the high M_w component is concentrated enough to be self-entangled in addition to the entanglement of low M_w component.[10,24] These measurements reveal that (a) the long chain dynamics not only depend on its weight fraction in the binary mixture but also systematically vary with the short chain length[24] and (b) elimination of the CR effect by embedding a trace amount of the probe chain in a matrix of higher molecular weight leads to[10] the recovery of the reptative scaling law $D_{tr} \sim M_w^{-2.0}$ for the center-of-mass diffusion coefficient D_{tr} of the probe chain, in direct conflict with the available simulation results.[13,14] These studies suggest that we should develop a more thorough understanding of chain dynamics in the dilute limit where the matrix (i.e., the solvent) is made of entangled chains.

The alternative term for CR is tube reorganization: Beyond the relaxation time of matrix chains the probe chain behaves Rouse-like so that tube reorganizes as if it is executing Rouse dynamics. Previous studies have found evidence[15−17] for such behavior using polystyrene (PS), which has one of the largest entanglement molecular weights M_e among all polymers. When the trace long chain is sufficiently long in comparison to that of the matrix chain, even an entangled matrix could act like just a solvent in the sense that the long chain might obey Zimm dynamics, behaving like a Stokes sphere. This intuition was first suggested by Daoud and de Gennes[4] in 1979. In this case, the probe chain dynamics are similar to those in conventional small molecule solvents. The PS samples used in the previous studies[15−17] were too short to be in this Stokes-sphere regime. The IR diffusion study[18] on 1,4-PBD cannot probe the Stokes-sphere regime either because the diffusion time would be unrealistically long.

In the present paper, we explore the probe chain dynamics as a function of both matrix and probe chain

* Corresponding author. E-mail: swang@uakron.edu.

10.1021/ma0489669 CCC: $30.25
Published on Web 12/15/2004

lengths using 1,4-PBD as a model system. Specifically, we are interested in mapping out the theoretically anticipated different regimes including a familiar Zimm solution region based on small molecule solvents, a Rouse-like region for nonentangled matrices, a constraint-release active "hindered Rouse" region for entangled matrices, and a Stokes-sphere region. As indicated above, no experimental evidence has been found of the Stokes-sphere region because the previous diffusion measurements were impractical to access the Stokes dynamics.

Since the Stokes-sphere region involves a very long chain, the available techniques to make diffusion measurements are further rendered nearly useless because neither force recoil spectroscopy nor IR spectroscopy has the sensitivity to detect the diffusing component in the dilute solution limit where the volume fractions are below the overlapping concentration, which can be very low, e.g., below 1%, for sufficiently long chains. We recognize that solution rheological characterization is perhaps a uniquely sensitive tool suitable to explore the remaining unexplored part of the dynamic phase diagram. In this work, we propose to carry out rheological measurements to interrogate the dilute solution dynamics associated with a trace amount of long chains in a matrix of short chains that can be either entangled or not.

In this paper, we outline the theoretical predictions using simple scaling analyses without numerical prefactors, describing not only the boundaries between the different dynamical regimes but also the rheological characteristics that can be used to identify these dynamics. Then we present data from linear viscoelastic measurements carried out in both the dilute limit and the entire concentration range so that the onset of semidilute regime can be readily identified, and the shift of chain dynamics can be revealed from Zimm-like to Rouse-like as the concentration increases.

II. Theoretical Outline

Non-Entangled Matrix ($N_M < N_e$). When the matrix chains (M) are not entangled, the probe chain (P) dynamics can be either the familiar Zimm solution like or Rouse-like, depending on the relative chain lengths N_M and N_P. The appendix of ref 24 provided a brief account of respective dynamics and the condition separating them, which can be generalized to allow hydrodynamic draining:

$$\frac{D_Z}{D_R} = \left(\frac{N_P}{N_M}\right)\frac{b}{R_H} \sim 1 \qquad (1)$$

where D_Z and D_R are the self-diffusion coefficients of the probe chain, corresponding to Zimm and Rouse dynamics respectively and the hydrodynamic radius R_H scales as N_P^{θ} with the exponent θ between the Gaussian value of $^1/_2$ for a Θ solvent (i.e., $R_H = R_P = b\sqrt{N_P}$) and the Flory exponent $^3/_5$ for good solvent in absence of draining. This condition holds for both $N_P < N_e$ and $N_P > N_e$ and can be simply indicated in a dynamic phase diagram as shown in Figure 1, where for simplicity the ideal case of $\theta = ^1/_2$ is given.

Entangled Matrix ($N_M > N_e$). Since the matrix chains are entangled, the probe chain cannot freely diffuse around without encountering entanglement with the matrix chains. The idea of constraint release (CR) has been proposed to reflect the ability of the tube to reorganize and the probe chain to move Rouse-like.[3–5] In other words, beyond the time scale $\tau_d(N_M)$ of disentanglement for the matrix chains the probe chain would be able to wander freely (i.e., Rouse-like) over a distance on the order of the tube diameter a, which is related to N_e as $(a/b)^2 = N_e$. Now the probe chain can be perceived to move as a tube-like object made of (N_P/N_e) repeated units on an elementary time scale of $\tau_d(N_M)$. This motion is therefore referred to in the literature as tube reorganization or tube renewal.[1,2] We can readily arrive at the following expression of the diffusion coefficient D_{hR} for the *hindered* Rouse-like motion of the probe chain in an entangled matrix

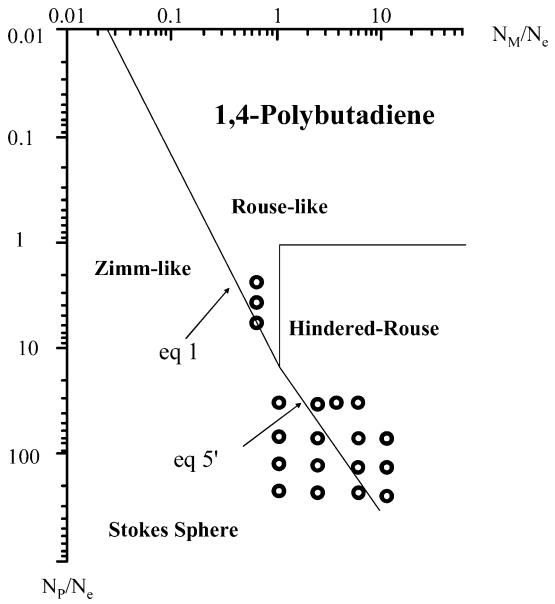

Figure 1. Partial dynamic "phase diagram" based on 1,4-polybutadiene mixtures in the dilute limit, with N_p and N_M being the probe and matrix chain lengths respectively, where the nineteen circles denotes the binary mixtures studied in this work. When the matrix chains are entangled, the probe chain dynamics can be either Rouse-like (i.e., hindered Rouse) or Zimm-like (i.e., Stokes sphere).

$$D_{hR}(N_P,N_M) = \frac{a^2}{\tau_d(N_M)(N_P/N_e)} \qquad (2)$$

The relaxation time associated with this hindered Rouse chain can also be straightforwardly derived by analogy to the standard formula for Rouse relaxation time[2]

$$\tau_{hR}(N_P,N_M) = \tau_d(N_M)\left(\frac{N_P}{N_e}\right)^2 = \frac{R_P^{\,2}}{D_{hR}} \qquad (3)$$

where $R_P^2 = N_P b^2$ is the mean square end-to-end distance of the probe chain.

A different form of eq 2 can be obtained using the standard relation[2] $\tau_d(N_M) = \eta_M/G_N^0$, where the elastic plateau modulus G_N^0 is independent of chain length and related to the tube diameter a as

$$G_N^{\,0} = \frac{\rho_w RT}{M_e} = k_B T/a^2 b$$

We find

$$D_{hR}(N_P,N_M) = \frac{k_B T}{\eta_M b(N_P/N_e)} = \left(\frac{N_e}{N_M}\right)^3 D_R(N_P) \qquad (4)$$

Compared with the free Rouse diffusion coefficient

$$D_{\mathrm{R}}(N_{\mathrm{P}}) = \frac{k_B T}{\zeta N_{\mathrm{P}}}$$

this hindered Rouse diffusion coefficient D_{hR} is smaller by a factor of the cube of the number of entanglement points. Here we prefer to use the term "hindered Rouse" instead of "Rouse-like constraint release"[25] or tube Rouse because it is more explicit and intuitively meaningful.

When the probe chain length becomes increasingly long, the matrix chains may appear more like an ordinary solvent. In other words, the probe chain may eventually diffuse like a Stokes sphere. Compared with

$$D_{\mathrm{Stokes}}(N_{\mathrm{P}}) = \frac{k_{\mathrm{B}} T}{\eta_{\mathrm{M}} R_{\mathrm{H}}}$$

for Stokes spheres, eq 4 yields

$$\frac{D_{\mathrm{Stokes}}}{D_{\mathrm{hR}}} = \left(\frac{N_{\mathrm{P}}}{N_{\mathrm{e}}}\right)\frac{b}{R_{\mathrm{H}}} \sim 1 \qquad (5)$$

The boundary condition of eq 5 is similar to that given in eq 1 where the matrix is not entangled. A more sophisticated theoretical treatment[25] gives a slightly different form for eq 4, amounting to replacing N_{e} with $(N_{\mathrm{e}}N_{\mathrm{M}})^{1/2}$ in eq 5 so that

$$\frac{D_{\mathrm{Stokes}}}{D_{\mathrm{hR}}} = \left(\frac{N_{\mathrm{P}}}{\sqrt{N_{\mathrm{e}}N_{\mathrm{M}}}}\right)\frac{b}{R_{\mathrm{H}}} \sim 1 \qquad (5')$$

which recovers eq 29 of ref 25 when the probe chain is Gaussian and nondraining(i.e., $R_{\mathrm{H}} = R_{\mathrm{P}}$). Since the exponent θ for R_{H} has a lower bound of $^1/_2$, the borderline given by the dependence of N_{P} on N_{M} is stronger than linear. Like eq 1, this boundary condition can also be readily depicted in Figure 1.

Both diffusion and rheological measurements have been made to explore the probe chain dynamics in nonentangled[26] and entangled matrices.[15−18] The most extensively studied polymer is polystyrene. Because of the extremely high entanglement molecular weight M_{e} = 18 000 g/mol for PS, the available experimental techniques for the chosen molecular weights could only access the CR (i.e., hindered Rouse-like dynamics) region. The probe PS chain would have to be of an extraordinarily high molecular weight to enter the Stokes-sphere regime. The diffusion time in the Stokes-sphere regime is most likely unrealistically long for those techniques to apply. As for other polymers such as 1,4-polybutadiene and 1,4-polyisoprene, although sufficiently high molecular weight samples are readily available, the probe chain diffusion in the Stokes-sphere regime is also too slow to measure with the technique of IR spectroscopy. Thus, the region of the Zimm-like or Stokes-sphere dynamics has remained undetected experimentally. In absence of any experimental evidence for the predicted Stokes-sphere region, there has been an impression in the community that the constraint release leading to Rouse-like dynamics is a prevailing feature besides the reptation, as noted by Brochard-Wyart et al.,[25] where a much more complete dynamic phase diagram was presented.

To enter the Stokes-sphere requires a very long probe chain. Since the overlapping concentration decreases with the chain length, the dilute limit corresponds to a tiny amount of probe chains in a matrix. No experimental techniques based on diffusion measurements are sensitive enough to pick up the information associated with the diffusing probe chain. We suggest here that solution rheological characterization is perhaps uniquely suited to explore this part of the phase diagram. In the present work, we propose to carry out rheological measurements to interrogate the terminal dynamics associated with a trace amount of long chains in a matrix of short chains. Before embarking onto the experimental part, we first describe the rheological characterization the long probe chain dynamics in a matrix of short chains.

"Solution" Rheology of Long Chains in Short Chains. For nonentangled matrices ($N_{\mathrm{M}} < N_{\mathrm{e}}$), the viscosity increment $\Delta\eta$ due to the incorporation of the long chains depends on whether the long chain of length N_{P} would behave Rouse or Zimm-like. For Rouse dynamics, we have the following standard expression

$$\Delta\eta \equiv \eta - \eta_{\mathrm{M}} = G_{\mathrm{P}}\tau_{\mathrm{R}}(N_{\mathrm{P}}) \qquad (6)$$

where the solution modulus

$$G_{\mathrm{P}} = \frac{c\mathrm{R}T}{\mathrm{M}_{\mathrm{P}}} = \phi\left(\frac{\mathrm{N}_{\mathrm{M}}}{\mathrm{N}_{\mathrm{P}}}\right)G_0(N_{\mathrm{M}}) = \phi\left(\frac{\mathrm{N}_{\mathrm{e}}}{\mathrm{N}_{\mathrm{P}}}\right)G_{\mathrm{N}}{}^0 \qquad (7)$$

in the dilute limit at a concentration of $c = \phi\rho_{\mathrm{w}}$ or weight fraction of ϕ. Here we assume that the mass densities of long and short chains are the same, equal to ρ_{w}, $G_{\mathrm{N}}{}^0$ is the plateau modulus introduced just before eq 4, and

$$G_0(N_{\mathrm{M}}) = \frac{\rho_{\mathrm{w}}\mathrm{R}T}{\mathrm{M}_{\mathrm{M}}}$$

is the modulus of a nonentangled matrix. Writing eq 6 in terms of the matrix viscosity $\eta_{\mathrm{M}} = G_0(N_{\mathrm{M}})\tau_{\mathrm{R}}(N_{\mathrm{M}})$, we have

$$\Delta\eta = \phi\left(\frac{N_{\mathrm{M}}}{N_{\mathrm{P}}}\right)\left[\frac{\tau_{\mathrm{R}}(N_{\mathrm{P}})}{\tau_{\mathrm{R}}(N_{\mathrm{M}})}\right]\eta_{\mathrm{M}} = \phi\left(\frac{N_{\mathrm{P}}}{N_{\mathrm{M}}}\right)\eta_{\mathrm{M}}, \quad \text{Rouse-like for } N_{\mathrm{M}} < N_{\mathrm{e}} \qquad (8)$$

which indicates that the viscosity increment would be linearly proportional to the chain length N_{P}.

For entangled matrices, we are interested in distinguishing hindered-Rouse from Stokes-sphere dynamics in the dilute solution limit. In the hindered-Rouse limit, the expression for the viscosity increment $\Delta\eta$ is given by

$$\Delta\eta = G_{\mathrm{P}}\tau_{\mathrm{hR}}(N_{\mathrm{P}},N_{\mathrm{M}}) = \phi\left(\frac{N_{\mathrm{P}}}{\sqrt{N_{\mathrm{e}}N_{\mathrm{M}}}}\right)\eta_{\mathrm{M}}, \quad \text{hindered-Rouse for } N_{\mathrm{M}} > N_{\mathrm{e}} \qquad (9)$$

where use is made of eq 7 for G_{P}, eq 3 for τ_{hR} with

$$\mathrm{D}_{\mathrm{hR}} = \frac{k_{\mathrm{B}}T\sqrt{N_{\mathrm{e}}N_{\mathrm{M}}}}{\eta_{\mathrm{M}}N_{\mathrm{P}}b}$$

according to ref 25, and $G_{\mathrm{N}}{}^0 = k_{\mathrm{B}}T/a^2b$. This result not

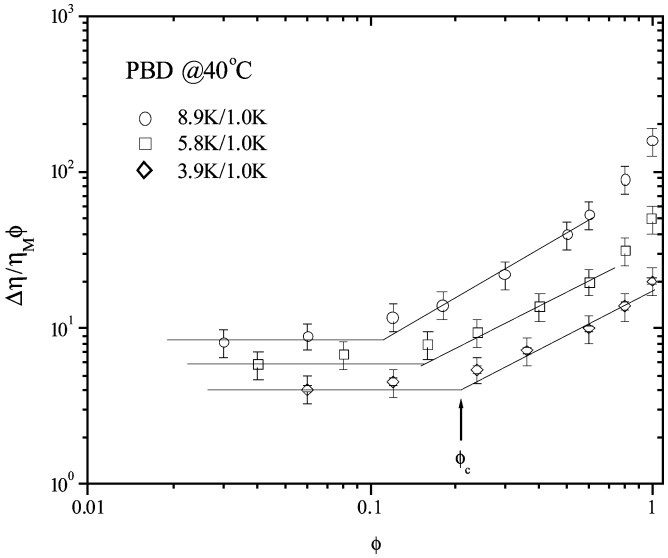

Figure 2. Normalized viscosity increment $\Delta\eta/\eta_M\phi$ as a function of weight fraction ϕ for binary mixtures of 8.9K, 5.8K, and 3.9K in the 1.0K matrix.

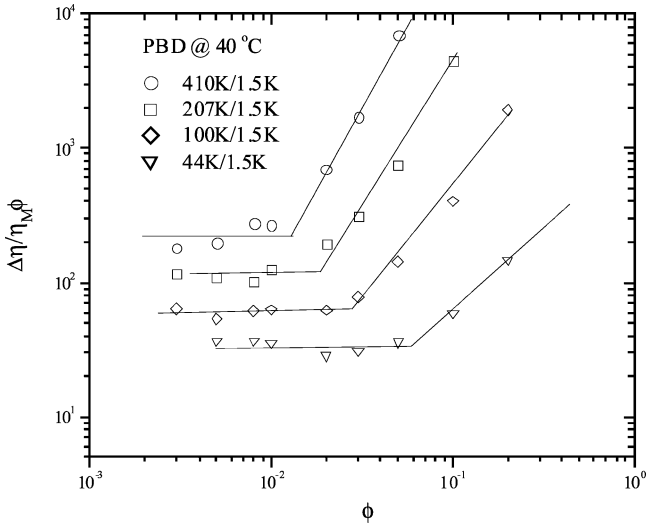

Figure 3. Normalized viscosity increment as a function of weight fraction ϕ for binary mixtures of 410K, 207K, 100K, and 44K in the 1.5K matrix, where the onset concentration ϕ_c is defined as indicated.

only is new but also disagrees with the previous result by Daoud and de Gennes[4] of

$$\Delta\eta = \phi\left(\frac{N_P}{N_e}\right)^2 \eta_M$$

The difference arises from the overestimate of the modulus G_P for dilute solutions by Daoud and de Gennes to invoke a simple mixing rule that amounts to having ϕG_N^0 instead of eq 7. Since the long chains are not mutually entangled with one another, the dilute solution modulus is only as high as given in eq 7, which is lower than that used in ref 4 by a factor of N_P/N_e. Our experimental data to be presented in the next section in Figure 6 are consistent with eq 9, where it is shown that the maximum dependence of $[\eta]$ on N_P is linear instead of quadratic.

Below the borderline depicted by eq 5′, we have the Stokes-sphere solution where the polymer chains are expected to be Zimm-like. For Zimm-like chains, we have the expression for the viscosity increment that

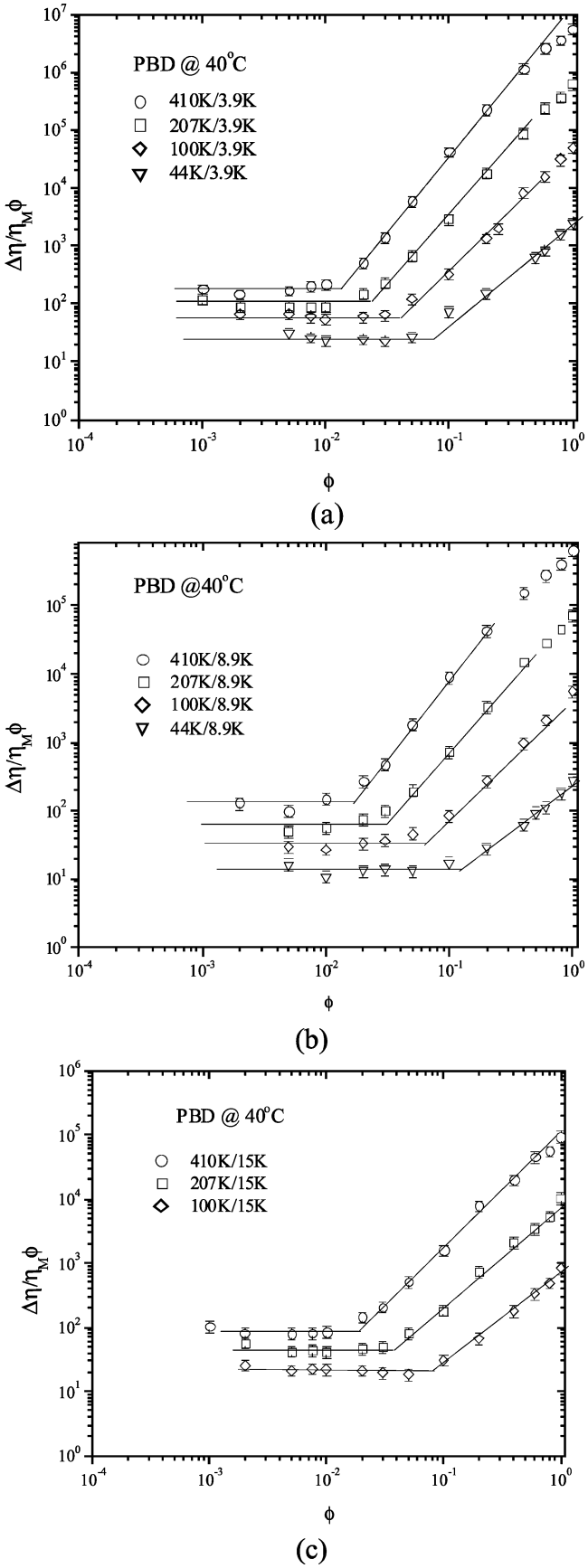

Figure 4. Normalized viscosity increment as a function of weight fraction ϕ for binary mixtures of 410K, 207K, 100K, and 44K in (a) the 3.9K matrix, (b) the 8.9K matrix, and (c) the 15K matrix, respectively.

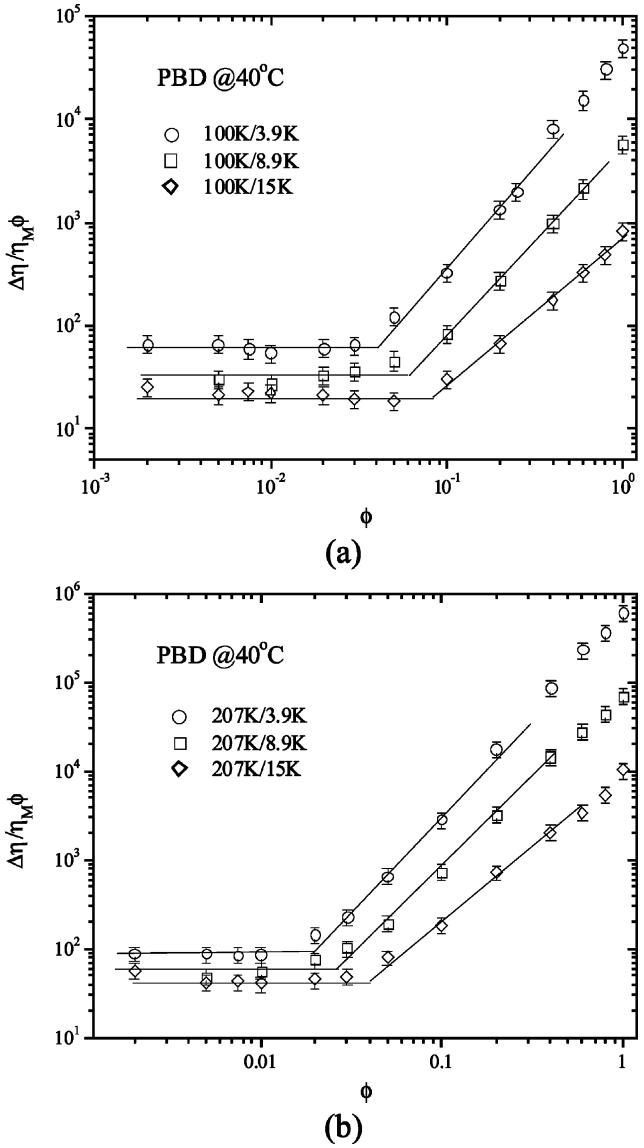

Figure 5. Normalized viscosity increment as a function of weight fraction ϕ for binary mixtures of (a) 100K and (b) 207K in matrices of molecular weight 3.9K, 8.9K, and 15K, respectively.

involves the knowledge of the Zimm-like chain relaxation time $\tau_Z(N_P) = R_H^2/D_{Stokes}(N_P)$

$$\Delta\eta = G_P\tau_Z(N_P) = \phi\left(\frac{R_H^3}{bR_P^2}\right)\eta_M, \quad \text{Zimm-like or Stokes-sphere} \quad (10)$$

This is a familiar result for Zimm chains in dilute solutions although it also represents a generalization of the original theory to include polymeric solvents.

III. Experimental Section

A. Sample Preparation. Our model mixtures are based on linear 1,4-polybutadiene (PBD) all synthesized and analyzed in the Goodyear Research Center through the courtesy of Dr. A. Halasa except for the last two samples in Table 1, one of which (PBD1.0K) was made at the University of Akron in Dr. R. Quirk's lab by Dr. J. P. Zhou and another one was purchased from Sigma-Aldrich Chemical Co. The synthesis was described in detail previously.[10] Table 1 shows the molecular characteristics of these samples, where all the samples are 1,4-PBD with a 1,4-content around 91% except

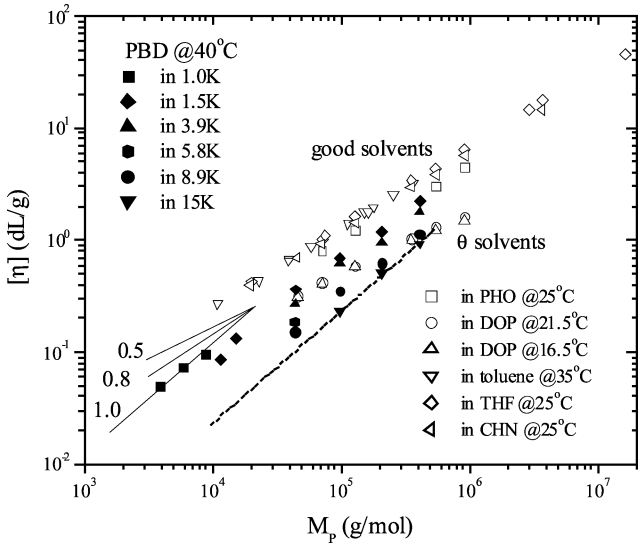

Figure 6. Intrinsic viscosity $[\eta]$ of dilute binary mixtures as a function of the probe chain molecular weight M_w for various matrix molecular weights as well as the literature values of $[\eta]$ for good and Θ solvents from refs 29−31, where the lower set of open symbols represents data based on Θ solvents.

Table 1. Molecular Characteristics of PBD Samples

sample	% 1,4	% 1,2	M_n	M_w	M_w/M_n	T_g (°C)
410K	92.3	7.7	411 000	412 000	1.01	−99.5
207K	91.9	8.1	207 000	208 000	1.01	−100.5
100K	91.8	8.2	98 900	99 100	1.01	−100.1
44K	91.7	8.3	43 500	43 900	1.01	−100.0
15K			14 000	15 500	1.10	
12K	91.4	8.6	11 300	11 600	1.03	−100.9
8.9K	91.4	8.6	8500	8900	1.04	−102.5
5.8K	91.0	9.0	5500	5800	1.06	−102.0
3.9K	90.1	9.9	3500	3900	1.10	−101.9
1.0K	90.0	10.0	900	1000	1.15	−105.4
1.5K	75.0	25.0		1500		−89.0

PBD1.5K, which has 75% 1,4-content and 25% 1,2-content. The binary mixtures under study consisted of a high molecular weight component and a low molecular weight component. The first set of samples was made of the long chains of PBD3.9K, -5.8K, and -8.9K respectively dispersed in a short chain of PBD1.0K. In the second set, the long chains are PBD with molecular weights 410K, 207K, 100K, and 44K, and the short chain solvents are PBD of lower molecular weights 15K, 8.9K, 3.9K, and 1.5K. Although the present study focuses on the chain dynamics in the dilute limit, the mixtures have been prepared at all concentrations from the dilute limit to the pure long chain melt. The mixtures are prepared by dissolving both the long and short chain melts in toluene. The dissolution normally took over 2−3 days in the dark at room temperature, with periodic manual stirring. After achieving a uniform solution, toluene was then removed under vacuum at room temperature for at least 1 week until the sample contains less than 0.2% of toluene.

B. Rheological Measurements. Linear viscoelastic properties of the PBD mixtures are measured by a dynamic mechanical spectrometer (Advanced Rheometrics Expansion System-ARES) at frequencies ranging from 0.1 to 100 rad/s and various temperatures between −40 and +40 °C. For most samples, experiments were carried out at temperatures higher than −40 °C to avoid crystallization of the low molecular weight PBD.[27] The spectrometer is equipped with a 200−2000 g·cm dual range, force rebalance transducer, and oscillatory shear measurements were carried out using a 25 mm diameter parallel plate flow cell. Gap settings of 0.5−1.0 mm were used. A small strain ($\gamma < 0.05$) is always used when $|G^*|$ is large, and no strain amplitudes are larger than 0.30.

Dynamic shear experiments are carried out to measure the storage and loss moduli G' and G'' of the binary mixtures

besides the zero-shear viscosity η_0. From the master curves for G' and G'', the frequency dependence of intrinsic moduli $[G']$ and $[G'']$ are constructed to elucidate the chain dynamics at various concentrations. The steady-state shear viscosities at low shear rate were also measured and the results are consistent with the dynamic viscosity at low frequencies. The measured η_0 at 40 °C for both pure melts and binary mixtures are shown in Table 2 (Supporting Information).

IV. Results and Discussion

In the current study, we choose 1,4-polybutadiene (PBD) to make binary mixtures. For PBD the boundary between CR regime and Stokes regime can be easily accessed. The PBD binary mixtures described in Table 2 (Supporting Information) are indicated in the phase diagram of Figure 1. Half of samples are expected to show Stokes behavior according to the theoretical dynamic phase diagram of Figure 1. On the other hand, the mixtures made of 3.9K, 5.8K, and 8.9K in 1.0K are expected to exhibit Rouse-like behavior. Molecular weight dependence of the intrinsic viscosity provides valuable information about the chain dynamics. We can also learn about the chain dynamics, i.e., Zimm-like vs Rouse-like, by determining intrinsic moduli $[G']$ and $[G'']$ and comparing with the predictions according to the standard bead−spring model for dilute polymer solutions.[28]

A. Viscosity of Mixtures. Nonentangled Matrix ($N_M < N_e$). Equation 1 indicates that when the probe chain length is not sufficiently long the matrix chains can screen the hydrodynamic interactions and make the probe chain dynamics Rouse-like. To verify this scaling prediction experimentally, we prepared dilute solutions made of PBD3.9K, -5.8K, and -8.9K in 1.0K. Figure 2 shows the viscosity increment $\Delta\eta = \eta - \eta_M$ as a function of the concentration. In the dilute limit where $\Delta\eta/\phi$ is constant represented by the horizontal lines, we see that $\Delta\eta$ essentially scales linearly with the probe chain length N_P, in agreement with eq 8. A crossover concentration ϕ_c is defined here as the beginning of the nonlinear dependence of $\Delta\eta$ on ϕ.

When the probe chain length is sufficiently long, a short-chain matrix is expected to act like a rather good solvent, allowing the probe chain to show Zimm dynamics. Figure 3 shows the solution viscosity as a function of the concentration for four different probe chain lengths. The viscosity increment $\Delta\eta$ scales with N_P more gradually than linearly, indicating typically Zimm-like solution behavior.

Entangled Matrix ($N_M > N_e$). 1. Dependence on Probe Chain Length. Rheological characteristics of binary mixtures have been obtained using oscillatory shear measurements of the zero-frequency shear viscosity. Figures 4a−(c) show the concentration dependence of the viscosity increment $\Delta\eta$ normalized by the matrix viscosity η_M for three different matrix chain lengths. As expected, the onset of nonlinear ϕ dependence of $\Delta\eta$ occurs at a lower concentration for a higher probe chain molecular weight. The explicit molecular weight dependence of the intrinsic viscosity $[\eta] = \Delta\eta/\rho_w\phi\eta_M$ will be analyzed in a subsequent subsection, where ρ_w is the mass density of the PBD. Note from Figure 4, parts a−c, that the viscosity increment changes with the probe chain molecular weight at most as strongly as linearly.

2. Dependence on Matrix Chain Length. As discussed in section II, the probe chain dynamics cross over from hindered Rouse to Stokes dynamics according to eq 5′ as the matrix chain length N_M varies. For a fixed probe chain length, its intrachain excluded volume and hydrodynamic interactions vary with N_M, which controls the matrix chains' ability to screen these interactions. Figure 5, parts a and b, illustrates how the viscosity increment for two probe chain molecular weights respectively depends on the matrix chain molecular weight. It is interesting to note not only how the magnitude of $\Delta\eta$ depends on N_M, as anticipated by eqs 9 and 10, but also how the onset of nonlinear ϕ dependence of $\Delta\eta$ shifts to higher values of ϕ for a larger N_M.

3. Intrinsic Viscosity. In summary, we present the intrinsic viscosity $[\eta]$ for the various binary mixtures obtained in the linear ϕ dependence regime as shown in Figure 6, where the literature data[29−31] are also included to provide the guide lines. There are a couple of important comments to make. The intrinsic viscosity varies systematically with the matrix molecular weight. For a given probe chain, the intrinsic viscosity is higher for a lower matrix molecular weight. For solutions based on 410K, the variation is within the boundaries of good and Θ solvents. Phenomenologically, this trend is consistent with the expectation that the screening of excluded volume interaction (EVI) is stronger for longer matrix chains.[1,32−35] It is known that the chain dimension and the second osmotic virial coefficient depend on the molecular weights of the both components in dilute polymer mixtures.[36] Scaling behavior of swollen chains in bimodal molecular weight blends has previously been studied by small-angle neutron scattering (SANS) to show the screening of EVI by the matrix chains.[37] Moreover, chain dimensions of polystyrene diluted with benzene, styrene monomer, and low molecular weight homologues have recently been measured using SANS to show[38] that the critical matrix chain molecular weight to eliminate the excluded volume effects is much higher than the theoretical prediction of eq 1 where a prefactor is omitted.

4. Boundary between Hindered Rouse and Stokes Sphere Dynamics. For several probe chain molecular weights, $[\eta]$ even drops significantly below the Θ-solvent line, i.e., $[\eta] < [\eta]_\theta$. In particular, the solutions based on the matrix of 15K are entirely below the reference points for Θ solvents. This indicates that apart from the shrinkage of the probe chain dimensions, which causes $[\eta]$ to drop, there is also a significant amount of screening of hydrodynamic interactions as the systems move across the boundary dividing the Stokes-sphere and hindered-Rouse regions. The mixtures below the Θ-solvent line include all based on the 15K matrix, the three points involving short probe chains in the 1.0K matrix, and the two points involving shorter probe chain lengths in the 1.5K matrix as well as several points based on the 8.9K matrix. The dependence on the probe chain length is linear for several of these Rouse-like solutions, which is consistent with the analysis given in eq 9 and in contradiction with the earlier prediction of Daoud and de Gennes.[4] For a given matrix such as 15K, the draining effect is stronger for a shorter probe chain. In other words, there is more screening of hydrodynamic interactions for the probe chain of molecular weight 100K than for 410K. Since the degree of draining varies with N_P, the observed linear dependence as depicted by the down-pointed triangles may not indicate the true Rouse-like behavior. In other words, there is in reality clearly no such sharp boundary as

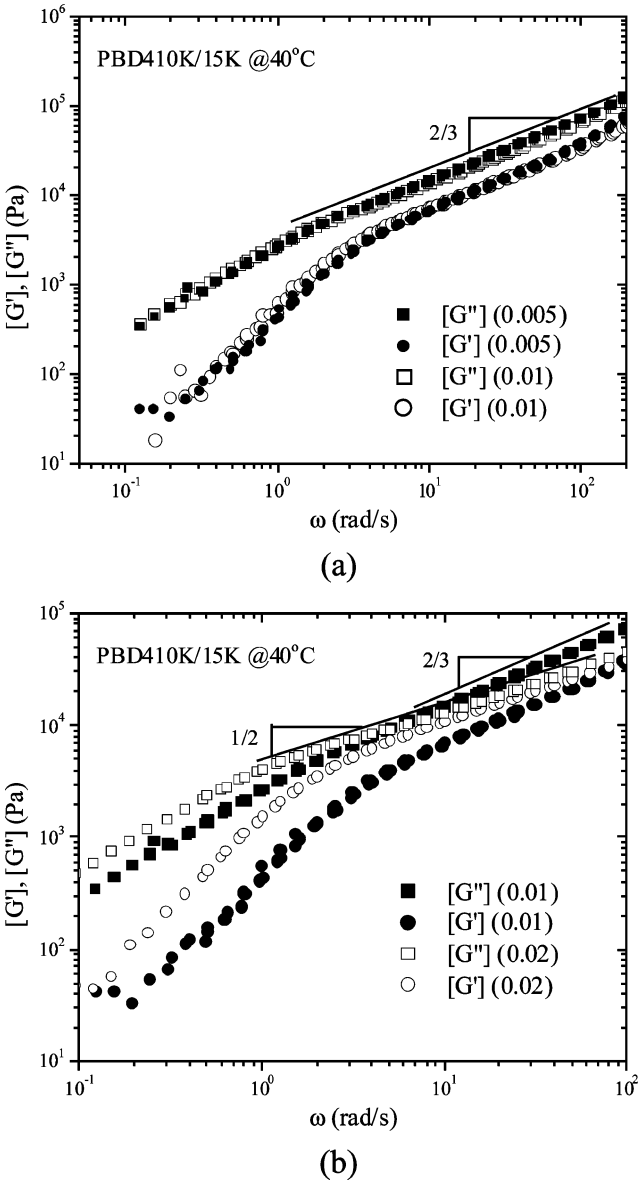

Figure 7. Intrinsic storage and loss moduli [G'] and [G''] of the 410*K*/15K mixtures (a) in the dilute limit corresponding to weight fractions of 0.005 and 0.01 and (b) comparison between Zimm-like and Rouse-like dynamics at $\phi = 0.01$ and 0.02, respectively.

depicted by eq 5′. To further investigate the chain dynamics in these mixtures, we carry out dynamic shear measurements as described below.

B. Intrinsic Dynamic Moduli. In this section, the characteristics of intrinsic moduli [G'] and [G''] are described to show further evidence of Stokes-sphere behavior, to explore the effect of the matrix molecular weight on the probe chain dynamics, and to elucidate the concentration effect. The intrinsic moduli [G'] and [G''] were evaluated from the G' and G'' of the mixtures according to[28]

$$[G'] = (G' - G'_M)/\phi,\ [G''] = (G'' - \omega\eta_M)/\phi, \quad \text{in the linear regime} \quad (11)$$

where G'_M is the storage modulus of the matrix, and it is negligible in the frequency range when the matrix chain molecular weight is much less than that of the probe chain.

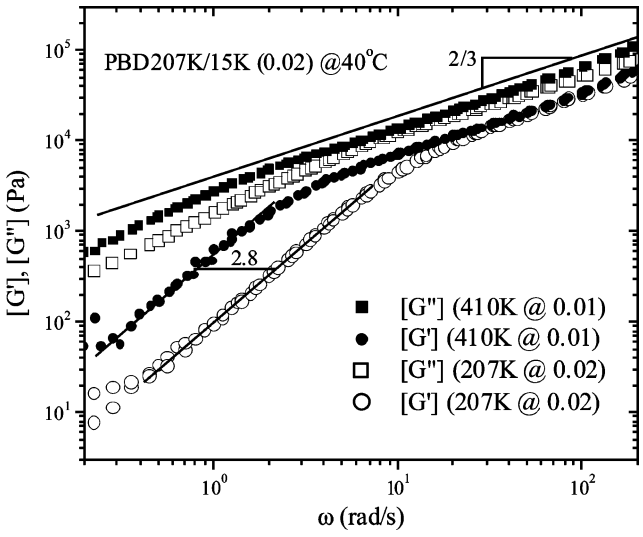

Figure 8. Intrinsic storage and loss moduli [G'] and [G''] of the 207K/15K mixture at a weight fraction of 0.02 in comparison with those of 410K/15K at $\phi = 0.01$.

In Figure 7a, the intrinsic moduli of PBD410K in 15K are presented as a function of frequency in the dilute limit, which is confirmed by the overlapping of the data. The observed scaling behavior of [G'], [G''] $\sim \omega^{2/3}$ is consistent with the Zimm theory. Even the separation between [G'] and [G''] of 2.0 is close to the Zimm prediction[28] of $\sqrt{3}$. This result suggests that the probe chain dynamics are close to the Stokes-sphere dynamics, where the 15K matrix appears to act like a Θ solvent. It is interesting to remark that as soon as the mixture moves away from the linear region into the semidilute regime, the probe chain dynamics turn decisively into Rouse-like dynamics with the scaling of [G'], [G''] $\sim \omega^{1/2}$ as shown by the comparison given in Figure 7b. At $\phi = 0.02$, the viscosity increment just starts to deviate from its linear ϕ dependence as shown in Figure 4c.

According to Figure 4c, the probe chain of molecular weight 207K in the 15K matrix is still in the dilute limit at $\phi = 0.02$. Figure 8 shows the intrinsic moduli for two different probe chain molecular weights at two different concentrations. The mixture of 207K/15K reaches the scaling regime of [G'], [G''] $\sim \omega^{2/3}$ at a frequency higher than the onset frequency for 410K/15K by a factor of 2.8 as indicated in Figure 8. This is consistent with the molecular weight dependence of the probe chain relaxation time $\tau_Z \sim M_w^{1.5}$ and implies that the chain dynamics are those of the Zimm-like Θ solution. Nevertheless, the corresponding intrinsic viscosity [η] for the dilute 207K/15K mixtures is visibly lower than the value for a Θ solution as shown in Figure 6, which is rather mysterious. Clearly, the present simple-minded scaling argument is incapable of explaining the double feature of [η] < [η]$_\theta$ and [G'], [G''] $\sim \omega^{2/3}$ in the dilute mixtures of 207K/15K. Also surprising is absence of any Rouse-like scaling for [G'], [G''] $\sim \omega^{1/2}$ in the dilute limit in any of the studied mixtures. It seems that a more detailed theory is required to account for the observed dynamic behavior.

C. Dependence of Crossover Concentration on N_P and N_M. To further elucidate the probe chain dynamics as a function of both matrix and probe chain lengths N_M and N_P, we examine the onset concentration ϕ_c, where the viscosity increment begins to vary more strongly than linearly with concentration. Reading ϕ_c from Figures 2, 3 and 4a−c, we plot ϕ_c against the probe

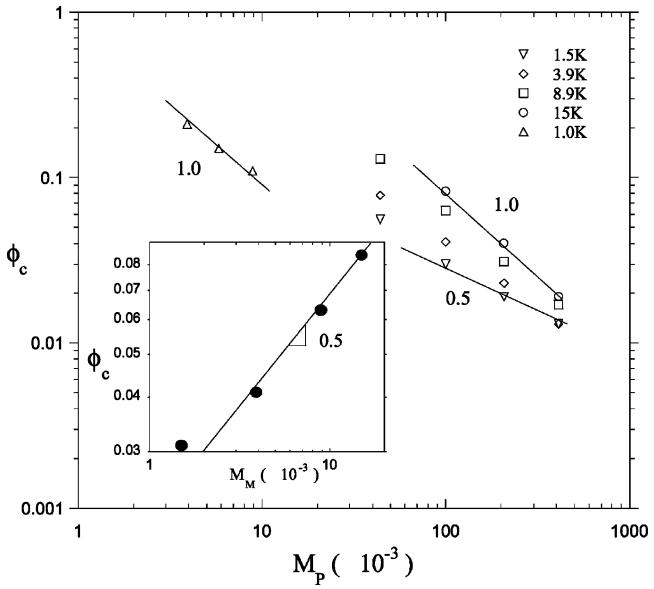

Figure 9. Onset concentration ϕ_c defined in Figure 2 as a function of the probe chain molecular weight for various matrix molecular weights, where the limiting scaling exponents of 0.5 and 1.0 are both indicated by the solid and dashed lines. The inset indicates for a probe chain molecular weight of 100K that ϕ_c increase with N_M with an exponent of 0.5.

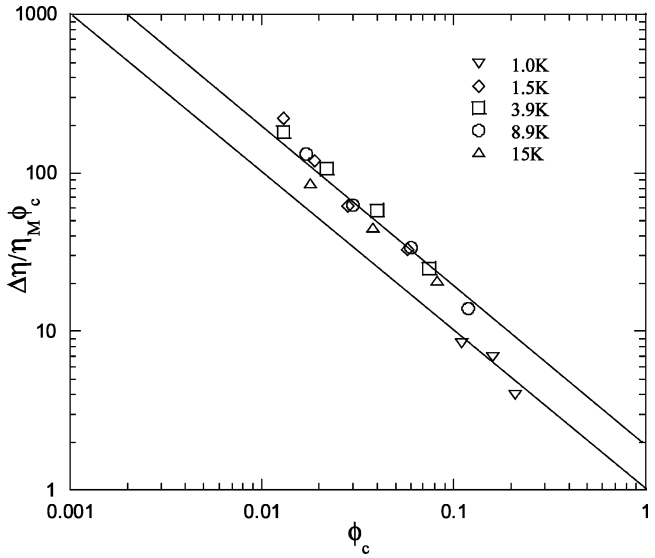

Figure 10. Viscosity increment at ϕ_c all the mixtures studied in Figures 2-5, where the diagonal line represents $\Delta\eta = \eta_M$, and the other line indicates $\Delta\eta = 2\eta_M$.

chain molecular weight as shown in Figure 9 for various matrix molecular weights. It is rather revealing to see that the scaling exponent n in $\phi_c \sim M_P^{-n}$ shifting from 0.5 to 1.0 as the matrix chain length increases. If we take ϕ_c as the overlapping concentration, the exponent n is expected to be 0.5 for a Θ Zimm solution. For n to be as large as 1.0 is unusual since Rouse dynamics in dilute solution has hardly ever been observed in the past. The physical meaning of ϕ_c is perhaps rather straightforward: at ϕ_c the viscosity increment $\Delta\eta$ becomes comparable to η_M. This means, according to eq 10, that

$$\phi_c\left(\frac{R_H^3}{bR_P^2}\right) \sim 1$$

for Zimm solutions, and according to eq 9 that

$$\phi_c\left(\frac{N_P}{\sqrt{N_e N_M}}\right) \sim 1$$

for Rouse-like solutions. So it seems that the mixtures based on the matrix of molecular weight 15K are more like Rouse solutions, whereas the mixtures made of the probe chain molecular weights equal to 410K and 207K in the 1.5 matrix are Zimm solutions. The other mixtures are perhaps between these two limiting types of dynamics. It is also striking to note that ϕ_c increases with matrix chain length as $\sqrt{N_M}$ as shown in the inset of Figure 9 in agreement with that anticipated by eq 9. Since R_H would decrease with increasing N_M due to screening of both hydrodynamic and excluded volume interactions eq 10 also expects ϕ_c to increase with N_M. Finally, it is worth mentioning that in all the cases shown in Figure 7a,b and Figure 8, G' and G'' turn Rouse-like, scaling as $\omega^{1/2}$ at high frequencies only when $\phi > \phi_c$.

It is straightforward to determine the value of specific viscosity $\Delta\eta/\eta_M$ at ϕ_c for all the solutions studied in this work. Figure 10 shows that except for the three Rouse solutions based on the 1.0K matrix all others have $\Delta\eta/\eta_M \sim 2.0$ at ϕ_c. There does seem to be a sign that the data points tend to approach the line of $\Delta\eta/\eta_M = 1.0$ as the matrix chain length increases.

V. Conclusions

There are several effects on the probe chain dynamics in a dilute binary mixture. For nonentangled matrices, the probe chain dynamics can switch from the familiar Zimm dynamics to Rouse-like behavior. For entangled matrices, the effective screening of the hydrodynamic interactions by the matrix chain typically leads to hindered-Rouse dynamics (more commonly known as Rouse tube reorganization). But the Zimm-like Stokes-sphere can reappear when the probe chains are sufficiently long. Using solution rheology as a uniquely valuable method we explore these dynamics based on model 1,4-polybutadiene mixtures. Our rheological measurements allow us to access for the first time the Stokes-sphere region in binary mixtures where both components are entangled in their respective pure melt states. There is also ample strong evidence for the unusual Rouse-like dilute solution behavior because a number of the dilute mixtures find their intrinsic viscosity below the lower bound for Zimm solutions under Θ conditions as shown in Figure 6. Our experimental data are one of the first to support the theoretical prediction given in eq 9, which is based on previous results from ref 25. Finally, the critical concentration ϕ_c, where the solution viscosity starts to increase nonlinearly with the probe chain volume fraction ϕ, is found not only to change with the probe chain length but also with the matrix chain length, indicating how the nature of the probe chain dynamics is modified by the matrix chain. These experimental results call for a more quantitative theoretical description of chain dynamics in homobinary mixtures where both long and short chains may be entangled. It is also desirable to carry out SANS measurements of the probe chain dimensions for these model binary mixtures as a function of the matrix chain length and weight fraction of the probe chain.

Acknowledgment. This work is supported, in part, by NSF Grant (DMR 01-96033). The authors appreciate helpful comments from the reviewers.

Supporting Information Available: Table 2, zero-shear viscosity of PBD mixtures at 40 °C. This material is available free of charge via the Internet at http://pubs.acs.org.

References and Notes

(1) de Gennes, P. G. *Scaling Concepts in Polymer Physics*; Cornell University Press: Ithaca, NY, 1979.
(2) Doi, M.; Edwards, S. F. *The Theory of Polymer Dynamics*, 2nd ed.; Clarendon Press: Oxford, England, 1988.
(3) Klein, J. *Macromolecules* **1978**, *11*, 852.
(4) Daoud, M.; de Gennes, P. G. *J. Polym. Sci., Polym. Phys. Ed.* **1979**, *17*, 1971.
(5) Graessley, W. W. *Adv. Polym. Sci.* **1982**, *47*, 68.
(6) Doi, M. *J. Polym. Sci., Polym. Phys. Ed.* **1983**, *21*, 667.
(7) Milner, S. T.; McLeish, T. C. B. *Phys. Rev. Lett.* **1998**, *81*, 725.
(8) Fuchs, M.; Schweizer, K. S. *Macromolecules* **1997**, *30*, 5133, 5156.
(9) Wang, S. Q. *J. Polym. Sci., Polym. Phys. Ed.* **2003**, *41*, 1589.
(10) Wang, S.; von Meerwall, E. D.; Wang, S. Q.; Halasa, A.; Hsu, W. L.; Zhou, J. P.; Quirk, R. P. *Macromolecules* **2004**, *37*, 1641.
(11) Lodge, T. P. *Phys. Rev. Lett.* **1999**, *83*, 3218.
(12) Frischknecht, A. L.; Milner, S. T. *Macromolecules* **2000**, *33*, 5273.
(13) Deutsch, J. M.; Madden, T. L. *J. Chem. Phys.* **1989**, *91*, 3252.
(14) Reiter, J. *Chem. Phys.* **1991**, *94*, 3222.
(15) Green, P. F.; Kramer, E. J. *Macromolecules* **1986**, *19*, 1108. Green, P. F.; Mills, P. J.; Palmstrom, C. J.; Mayer, J. W.; Kramer, E. J. *Phys. Rev. Lett.* **1984**, *53*, 2145.
(16) Monfort, J.-P.; Marin, G.; Monge, P. *Macromolecules* **1984**, *17*, 1551.
(17) Watanabe, H. *Prog. Polym. Sci.* **1999**, *24*, 1253 and references therein, especially, Watanabe, H.; Kotaka, T. *Macromolecules* **1987**, *20*, 530.
(18) von Seggern, J.; Klotz, S.; Cantow, H.-J. *Macromolecules* **1991**, *24*, 3300.
(19) Barsky, S. *J. Chem. Phys.* **2000**, *112*, 3450.
(20) Struglinksi, M. J.; Graessley, W. W. *Macromolecules* **1985**, *18*, 2630.
(21) Viovy, J. L.; Rubinstein, M.; Colby, R. H. *Macromolecules* **1991**, *24*, 3587.
(22) Doi, M.; Graessley, W. W.; Helfand, E.; Pearson, D. S. *Macromolecules* **1987**, *20*, 1900.
(23) Yang, X.; Wang, S. Q.; Ishida, H. *Macromolecules* **1999**, *32*, 2638. Yang, X. P.; Halasa, A.; Hsu, W. L.; Wang, S. Q. *Macromolecules* **2001**, *34*, 8532.
(24) Wang, S.; Wang, S. Q.; Halasa, A.; Hsu, W. L. *Macromolecules* **2003**, *36*, 5355.
(25) Brochard-Wyart, F.; Ajdari, A.; Leibler, L.; Rubinstein, M.; Viovy, J. L. *Macromolecules* **1994**, *27*, 803.
(26) Kubo, T.; Nose, T. *Polym. J.* **1992**, *12*, 1351.
(27) Colby, R. H.; Milliman, G. E.; Graessley, W. W. *Macromolecules* **1986**, *19*, 1261.
(28) Ferry, J. D. *Viscoelastic Properties of Polymers*, 3rd ed.; Wiley: New York, 1980.
(29) Colby, R. H.; Fetters, L. J.; Funk, W. G.; Graessley, W. W. *Macromolecules* **1991**, *24*, 3873.
(30) Colby, R. H.; Fetters, L. J.; Graessley, W. W. *Macromolecules* **1987**, *20*, 2226.
(31) Roovers, J. *Polym. J.* **1986**, *18*, 153.
(32) Manke, C. W.; McAdams, J. E.; Williams, M. C. *Makromol. Chem., Rapid Commun.* **1984**, *5*, 165.
(33) McAdams, J. E.; Williams, M. C. *Macromolecules* **1980**, *13*, 858.
(34) Kitade, S.; Takahashi, Y.; Noda, I. *Macromolecules* **1994**, *27*, 7397.
(35) Colby, R. H. *J. Phys. (Paris)* **1997**, *7*, 93.
(36) Kirste, R. G.; Lehnen, B. R. *Makromol. Chem.* **1976**, *177*, 1137.
(37) Landry, M. R. *Macromolecules* **1997**, *30*, 7500.
(38) Torikai, N.; Takabayashi, N.; Noda, I.; Suzuki, J.; Matsushita, Y. *J. Phys. Chem. Solids* **1999**, *60*, 1325.

MA0489669